Defect and Diffusion Forum
ISSN: 1662-9507, Vol. 451, pp 35-44
doi:10.4028/p-QT6oyp

Submitted: 2025-12-19
Revised: 2026-03-03
Accepted: 2026-03-03
Online: 2026-04-17

Interfacial Welding of Two Different Reinforced Thermoplastics via TACOMA*

Katerina Vrettos[1,a], Steven Le Corre[1,b], Jean-Luc Bailleul[1,c*], Erwan Bertevas[2,d]

[1]Nantes Université, CNRS, Laboratoire de thermique et énergie de Nantes, LTEN, UMR 6607, F-44000 Nantes, France

[2]Nantes Université, IRT Jules Verne, F-44000 Nantes, France

[a]Ecaterini.Vrettos@univ-nantes.fr, [b]steven.lecorre@univ-nantes.fr,
[c*]Jean-luc.bailleul@univ-nantes.fr, [d]erwan.bertevas@irt-jules-verne.fr

*TACOMA for Thermo-Adhesion by Conductive heating of composite Materials

Keywords: interphase characterization, PEEK / LM-PAEK, welding thermoplastics.

Abstract. Thermoplastic composites offer new opportunities for multifunctional lightweight structures through their ability to be joined by fusion welding. However, the welding of dissimilar thermoplastic composites remains challenging due to asymmetric melting behavior and heterogeneous reinforcement architectures, all of which influence interfacial quality and mechanical performance. Within the CONNECT project, this study focuses on the adhesion development between a short carbon fiber reinforced PEEK and a continuous carbon fiber reinforced LM-PAEK laminate. Welding was performed using the TACOMA platform, which allows precisely controlled and asymmetric conductive heating cycles. The influence of welding temperature and contact time on interface formation was examined through Double Cantilever Beam (DCB) tests under Mode I loading, complemented by surface topography and scanning electron microscopy. Results show that welding at 350 °C significantly enhances interfacial fracture toughness compared to 345 °C, reflecting increased chain mobility of the PEEK matrix while the LM-PAEK phase is already molten. However, prolonged contact times lead to reorientation of short fibers parallel to the interface within the molten PEEK suppressing fiber bridging mechanisms at the interface and reducing the resistance to crack initiation, resulting in lower measured GIC values. These findings provide new mechanistic insight into the welding of dissimilar PAEK-based composites and identify a narrow processing window in which asymmetric melting and reinforcement morphology jointly govern interfacial performance. The interfacial fracture toughness was evaluated using a mode I initiation energy approach, selected due to unstable crack propagation in this bi-material configuration.

Introduction

High-performance thermoplastic polymers have emerged as attractive alternatives to thermosetting matrices in advanced composite structures. Among them, poly (aryl ether ketones) (LM-PAEKs) forms a family of semicrystalline polymers renowned for their excellent thermal stability, solvent resistance, and mechanical performance [1]. Within this family, polyether ether ketone (PEEK) has gained particular attention for its ability to be processed into composites with outstanding strength and toughness [2].

In demanding sectors such as aerospace and aviation, LM-PAEK and PEEK-based composites are increasingly adopted owing to their high strength-to-weight ratio, damage tolerance and reusability. However, composite assemblies remain challenging because local stress concentrations near fasteners can initiate damage and compromise structural integrity [3]. This limitation underscores the need for joining techniques that minimize mechanical fastening.

Thermoplastic matrix composites (TMCs) address this challenge, as they can be joined by welding. Unlike thermosets, thermoplastics lack chemical crosslinking and can therefore be remelted and reshaped. When heated above the melting temperature under pressure, molecular chains interdiffusion

across the interface and form new entanglements, resulting in joint healing [4]. This characteristic makes PAEK-based composites highly suitable for welded structures [5,6].
Nevertheless, the same features that make LM-PAEKs high-performance materials-rigid aromatic backbones, high crystallinity, and elevated melting points—also render them difficult to weld efficiently. Successful welding requires heating close to or above the melting point of the adherends while ensuring intimate contact and sufficient pressure to promote chain mobility [8]. Although progress has been achieved in fusion-welding techniques such as induction, resistance, and laser welding, most studies have focused on identical material systems (e.g., PEEK–PEEK or PEKK–PEKK) [9]. Welding of dissimilar PAEK-based composites remains far less explored, despite its industrial relevance.
Hybrid joints between short-fiber-reinforced PEEK and unidirectional continuous-fiber LM-PAEK offer a promising approach, combining the high stiffness and load-bearing capacity of continuous fibers with the design flexibility and cost efficiency of injection-molded short-fiber composites [6,7]. The presence of short fibers near the interface may promote crack deflection, mechanical interlocking or localized stress concentrations, strongly influencing fracture behavior.
In this context, this study investigates the welding of two dissimilar thermoplastic composites, emphasizing how asymmetric melting and short fiber morphology govern the interface formation and fracture behavior of the welded joints.

Materials and Sample Preparation

Two different thermoplastic composites were employed in this study. The first was a laminate made of 24 plies of unidirectional continuous carbon fiber tape embedded in an LM-PAEK matrix (Tm ≈ 307 °C). The second was an injection-molded plate of short carbon fiber-reinforced PEEK (Tm ≈ 343 °C).
The injection-molded plates were cut into 125 × 25 mm specimens with a Protomax waterjet machine (Fig.1), to fit the TACOMA welding system size. A countersunk hole was drilled 6 mm from one end to accommodate a loading pin for fracture testing. Prior to welding, all specimens were cleaned with acetone and dried overnight at 180 °C to remove residual moisture. A 20 µm aluminum foil was inserted between the adherends at a distance of 50–60 mm from the loading point to define an initial crack, and polyimide tape was applied on the composite side in contact with the mold to facilitate demolding after welding.

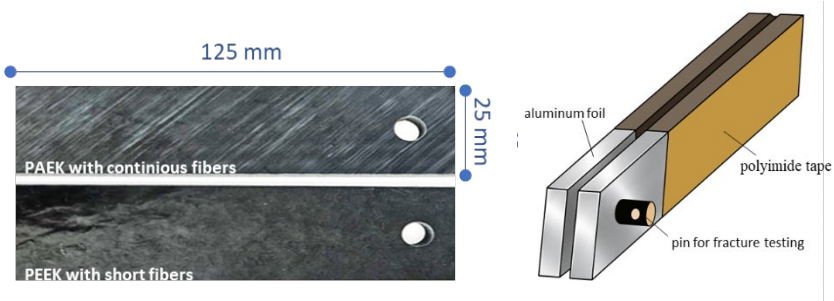

Fig. 1. Schematic illustration of the samples.

Experimental Welding Bench

The isothermal welding procedure performed on the TACOMA device (Fig.2) - originally developed for similar-material joints-has been previously described in detail by Avenet et al. [10]. The system consists of heated metallic plates equipped with embedded thermocouples and water-cooling channels, enabling precise control of time, temperature, and pressure. In this study, welding was achieved by heating both adherends to temperatures above their respective melting points, applying pressure for the selected contact time, and subsequently cooling under pressure to consolidate the interface. The welding pressure was determined through preliminary trials on the same hybrid configuration, which showed that higher pressures led to excessive flow and material loss of the

lower-melting LM-PAEK due to the combined effects of temperature and pressure, whereas lower pressures resulted in insufficient intimate contact. The selected pressure therefore ensured stable interface formation while minimizing polymer squeeze-out. All welding parameters used in the present study are summarized as follows: welding temperatures of 345 °C and 350 °C, constant pressure of 0.2 bar, and contact times ranging from 0 s corresponds to press closure at the target welding temperature followed immediately by the cooling stage, without any dwell time under pressure, to 200 s. The thermal cycle included heating, stabilization, contact under pressure, cooling under constant pressure, and pressure release (Fig.3).

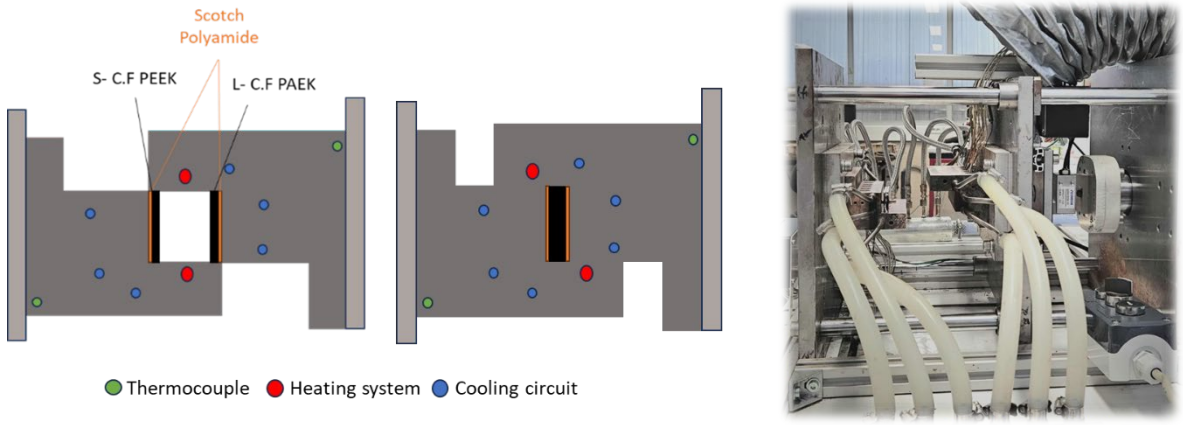

Fig. 2. Schematic representation of TACOMA before and during welding, showing specimens positioning and applied pressure and photograph of the actual instrumentation.

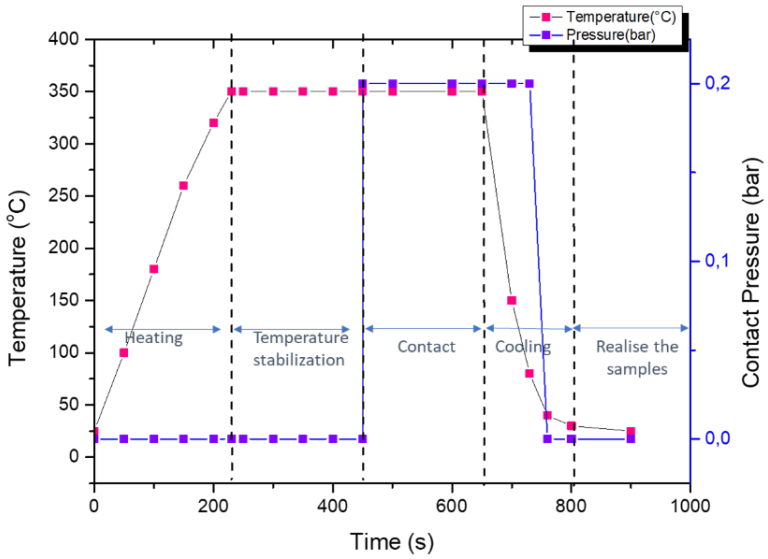

Fig. 3. Representative experimental welding cycle performed using the TACOMA conductive heating platform. The sequence includes heating to the target temperature (T_{weld} = 350 °C), temperature stabilization, contact under pressure (P = 0.2 bar) for $t_{contact}$ = 200 s, cooling under constant pressure, and final pressure release. An identical thermal sequence was applied for all specimens, with the welding temperature and contact time varied according to the processing parameters summarized in Table 1.

Table 1. Welding parameters tested in this study.

Temperature (°C)	Pressure (bar)	Contact Time (s)	Replicates
345	0.2	0–200	n=3
350	0.2	0–200	n=3

Fracture Testing

Double Cantilever Beam (DCB) tests were carried out on a 100 kN Zwick/Roell universal testing machine under displacement control at a constant crosshead speed of 1 mm·min^{-1}. Custom-designed loading pins were manufactured in-house and directly inserted into the pre-drilled holes of the specimens (Fig.4). The pins were carefully centered along the specimen width to ensure symmetric load transfer and to prevent torsional effects during testing. Load and displacement were continuously recorded throughout the experiment. The initial crack length a_0 was defined by the position of the 20 µm non-adhesive aluminum insert (50–60 mm from the loading point) and measured prior to testing. All tests were performed at room temperature (≈23 °C). For each welding condition, at least n = 3 specimens were tested to ensure repeatability. Since no standardized procedure currently exists for determining the interfacial fracture energy (G_{IC}) in such hybrid configurations, several data-reduction methods were evaluated. Among these, the Compliance Calibration Method (CCM) was initially considered more suitable for bi-material interfaces, as it accounts for differences in stiffness and compliance between the adherends [11].

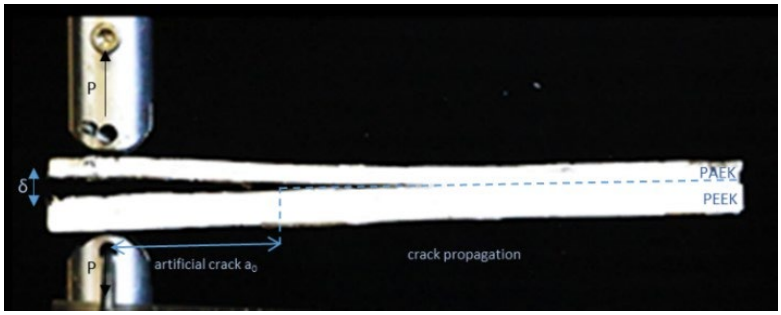

Fig. 4. Double Cantilever Beam (DCB) fracture test set-up.

The compliance method is expressed as:

$$G_{IG} = \frac{P^2}{2b}\frac{dC}{da} \quad (1)$$

where C=δ/P is the compliance, a is the crack length, P is the applied load, and b is the specimen width. For each crack length, compliance values were obtained from the force–displacement (F–δ) data. The derivative dC/da was determined through compliance calibration, where the compliance–crack length (C–a) relationship was fitted with a cubic polynomial ($C=C_3a^3+C_2a^2+C_1a+C_0$) to account for crack rotation and shear effects.

However, during the experiments, crack propagation was observed to be abrupt and unstable, preventing the establishment of a reliable compliance–crack length (C–a) relationship. As crack growth occurred over a very short time interval, it was not possible to accurately measure successive crack lengths (a_1, a_2, etc.) required for the application of the Compliance Calibration Method (CCM). Since CCM relies on stable and gradual crack propagation to ensure accuracy, this method was therefore not applicable under the present testing conditions.

It should be emphasized that no standardized procedure currently exists for the determination of mode I interfacial fracture toughness in hybrid thermoplastic composite systems involving adherends with distinct stiffness and reinforcement architectures. The present work therefore adopts an initiation energy approach as a pragmatic and physically consistent metric for comparative purposes. Ongoing work aims to establish a more robust methodology adapted to such asymmetric configurations.

Based on these observations, the classical Initiation Energy approach was adopted for the determination of the mode I interfacial fracture toughness G_{IC}. This approach evaluates the energy required to initiate crack propagation at the critical load and does not rely on stable crack growth or on the establishment of a compliance–crack length relationship. In the present hybrid configuration, involving two adherends with distinct mechanical properties and stiffness, crack propagation is strongly influenced by mechanical mismatch and stiffness asymmetry, making compliance-based approaches particularly sensitive to unstable fracture behavior. In contrast, the initiation fracture energy provides a well-defined and physically meaningful measure of interfacial resistance, as it is

governed by the onset of crack propagation rather than its subsequent evolution, thereby enabling consistent comparison between specimens processed under different welding conditions.
In this case, a_0 represents the initial crack length introduced by the aluminum foil between the adherends, P_c is the critical force required to initiate the crack, and δ_c is the corresponding displacement. The initiation fracture energy was calculated using Eq. (2).

$$G_{IC} = \frac{3P_c\delta_c}{2ba_0} \quad (2)$$

Overall, despite the lack of stable crack growth, the Initiation Energy approach proved to be a robust and physically justified method for assessing and comparing interfacial fracture toughness in this bi-material system, as it relies on a well-defined energy criterion at crack initiation that is not affected by the asymmetric stiffness and mechanical mismatch between the two adherends.

Materials Characterization

After the DCB fracture tests, the welded surfaces of the laminates were examined to study the failure mechanisms and the quality of the interface. First, optical inspection was carried out with a Keyence VHX-7000 digital microscope, which provides high-resolution images with magnifications up to 2000×.
The fracture surfaces were then analyzed in more detail using scanning electron microscopy (SEM) to observe their microstructural features. Finally, the surface roughness of the adherends before welding was measured with an ALICONA Infinite Focus 3D profilometer, which generates precise 3D maps of the surface topography. These measurements helped to evaluate how the reinforcement of the composites may affect the welding quality.

Results and Discussion

Fig. 5a shows the evolution of G_{IC} with contact time for both processing temperatures. An overall increase in G_{IC} is observed at 350°C, confirming that higher temperature enhances chain mobility and interdiffusion across the interface. At short contact times (10–20 s), the difference between specimens remains within the experimental scatter, suggesting that adhesion development is mainly governed by the establishment of surface contact rather than extensive molecular reptation. Among the investigated conditions, welding at 350 °C with short-to-intermediate contact times (10–20 s) yielded the highest measured initiation fracture toughness and is therefore identified as the optimal processing window within the explored parameter space.
In the present study, short contact times refer to 10s, and long contact times to > 20 s. At longer holding times, a noticeable decrease in G_{IC} is recorded for both temperatures. Image observations reveal that during prolonged exposure, the short fibers tend to reorient parallel to the interface rather than penetrating into the LM-PAEK matrix. As a result, they no longer act as mechanical bridges across the joint, leading to a reduction in effective load transfer at the onset of crack growth and consequently lower measured initiation fracture toughness. This morphological evolution explains the apparent drop in G_{IC} despite the longer contact duration.
To better correlate the interfacial strength evolution with the molecular interdiffusion process, the Degree of Healing (Dh) was computed from Eq. (3) using the measured mode I fracture toughness values G_{IC} normalized by the highest measured fracture toughness value obtained in this study, taken as the fully healed condition. The faster increase in Dh at 350°C reflects enhanced interfacial diffusion associated with increased chain mobility of the PEEK matrix, while the LM-PAEK phase is already fully molten. At 345°C, the healing remains incomplete (Dh ≈ 0.7), indicating that limited chain mobility of the PEEK restricts interfacial entanglement. The asymmetric melting behavior of the two polymers thus governs the observed healing kinetics, defining an optimal processing window near 350°C and short-to-moderate holding durations.

$$D_h = \sqrt{\frac{GIC}{GIC,\infty}} \quad (3)$$

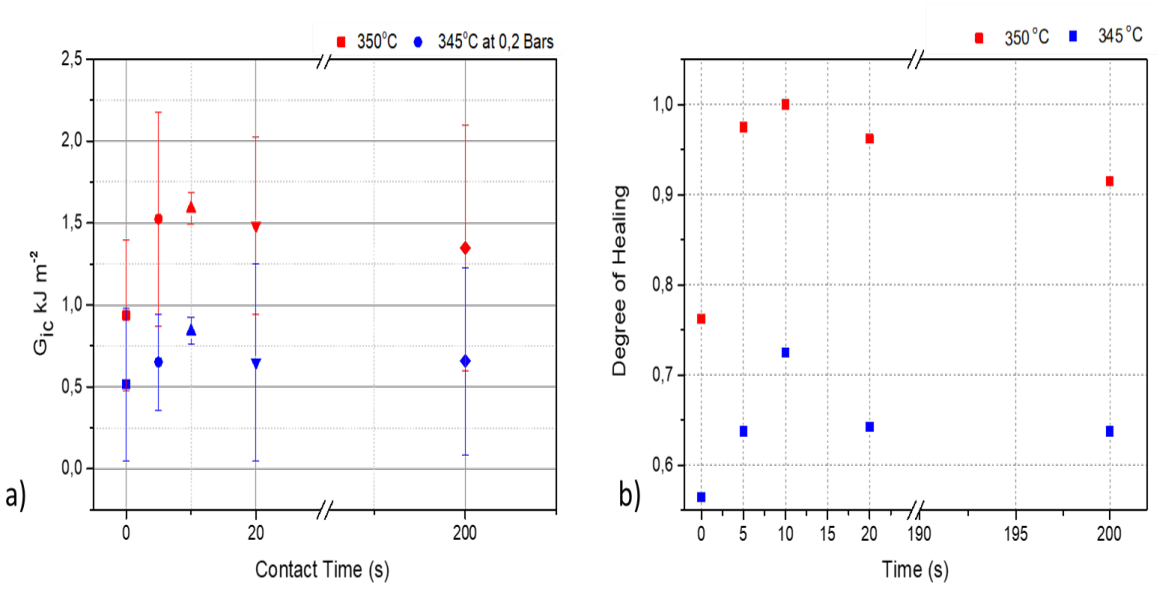

Fig. 5. a) Evolution of interlaminar fracture toughness for two isothermal temperatures versus contact time and b) Evolution of the Degree of Healing as a function of healing time for LM-PAEK/PEEK interfaces at 345 °C and 350 °C.

Observation of the Interface

This section presents a qualitative analysis of the cross-sections and fracture interfaces after the DCB tests, in order to study adhesion and material behavior under Mode I loading. Particular attention is given to the role of the short carbon fibers in the injection-molded PEEK adherend. Their presence at or near the welded interface can promote crack deflection, fiber bridging, or localized stress concentrations, thereby influencing the apparent fracture toughness.
Inspection of the fracture surfaces provides further observations that clarify how the crack propagates, whether failure occurs mainly at the interface or within the bulk material, and how short fibers contribute to the overall welding performance.

Profilometry, Micrographs and SEM Images

Fig. 6 illustrates the surface condition of the adherends before and after DCB testing. In Fig. 6a, the surfaces of the specimens prior to testing appear relatively smooth and homogeneous, without large defects or noticeable imperfections that could dominate crack initiation for both materials. After fracture (Fig. 6b), the surface shows clear evidence of crack propagation along the interface, with local damage zones and short fiber imprints. These features indicate a mixed failure mechanism combining adhesive and cohesive contributions. In Fig. 6b$_1$ we can observe the short fibers of PEEK attached on the surface of LM-PAEK and in Fig.6b$_2$ we can observe the hole they leave behind. Fig. 6c$_1$, obtained by optical microscopy, reveals that fragments of the PEEK matrix reinforced with short fibers remain attached to the LM-PAEK surface after fracture. This observation confirms that part of the failure occurred within the bulk PEEK material, providing direct evidence of cohesive failure. Such behavior highlights the contribution of short fibers to the crack path and to the overall welding performance.

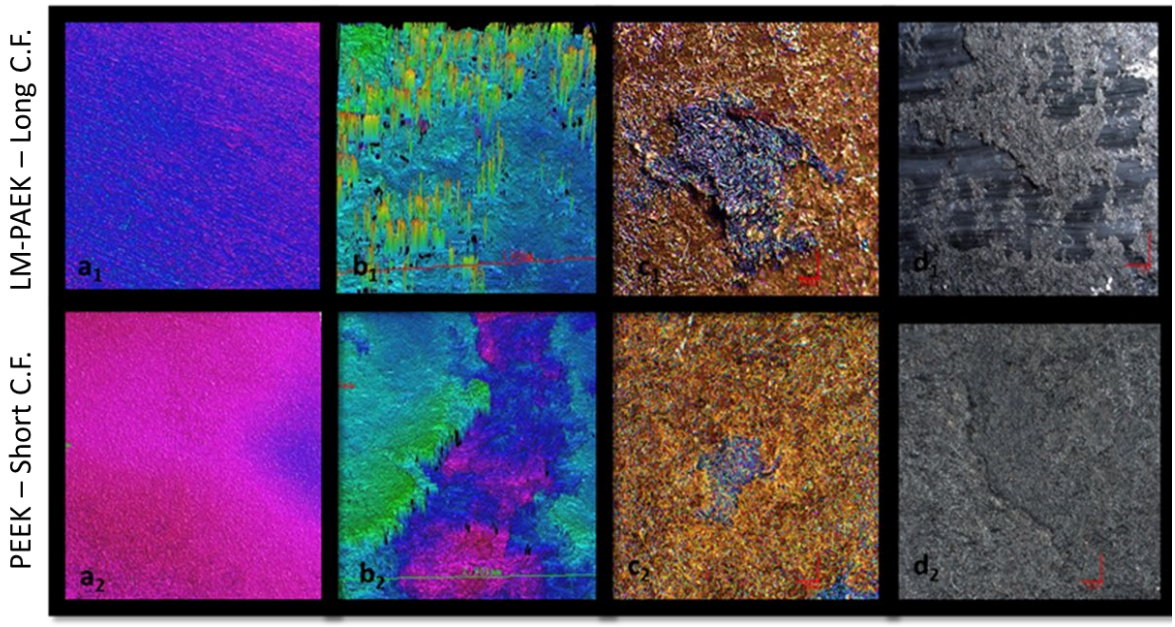

Fig. 6. a, b) Images of profilometry before and after healing and DCB test for both materials. c, d) Micrographs for both sides after DCB test. Sample welded at 350°C in 10s with 0.2 bar pressure.

The SEM observations corroborate the mechanical findings: specimens showing higher G_{IC} (350 °C) exhibited well-consolidated interfaces and partial fiber bridging. Fig. 7 presents images of the cross-section at the bonded interface prior to DCB testing. The overall welding line between the LM-PAEK laminate and the injection-molded PEEK plate is observed. The two adherends appear well joined, with no large voids or delamination zones, indicating good consolidation during welding. In the second image, a closer view of the interface highlights the transition zone between the continuous-fiber laminate and the short-fiber-reinforced PEEK. The presence of short fibers near the welding line is evident, suggesting that they can directly influence the interfacial morphology by promoting local mechanical interlocking and potentially altering crack initiation paths during loading. Fig. 8 shows SEM images of the fracture surfaces after DCB tests. In Fig.8a, the overall fracture surface of the LM-PAEK adherend reveals regions of interfacial failure combined with PEEK-rich areas. Fig. 8b and 8c provide higher magnifications, showing fiber imprints and short-fiber pull-out from the PEEK side. These features confirm mixed failure mechanisms: adhesive failure at the interface and cohesive fracture within the PEEK matrix. Fig. 9 presents images from cross-section of welded joints for 10s and 200s. It can be observed the short fibers penetrate into the opposing surface, acting like bridges for short contact times and the reorientation of the fibers at the interface without penetration on the matrix for longer contact times.

The combination of results from all characterization methods provides a comprehensive picture of the adhesion mechanisms in the welded joints. Before testing, the adherend surfaces appeared homogeneous and well-prepared, with no major defects at the interface. After DCB testing, the fracture occurred through a mixed mode, at the interface and cohesive failure within the PEEK matrix. The presence of short carbon fibers in the injection-molded PEEK played a decisive role: in some regions they enhanced adhesion through mechanical interlocking and crack deflection, while in others they acted as initiation sites for fiber pull-out. This dual effect explains the variability of the fracture surfaces and highlights the sensitivity of the welding performance to microstructural features. Overall, the observations confirm that interfacial adhesion in dissimilar thermoplastic composites is governed not only by processing conditions but also by the intrinsic morphology of the adherends.

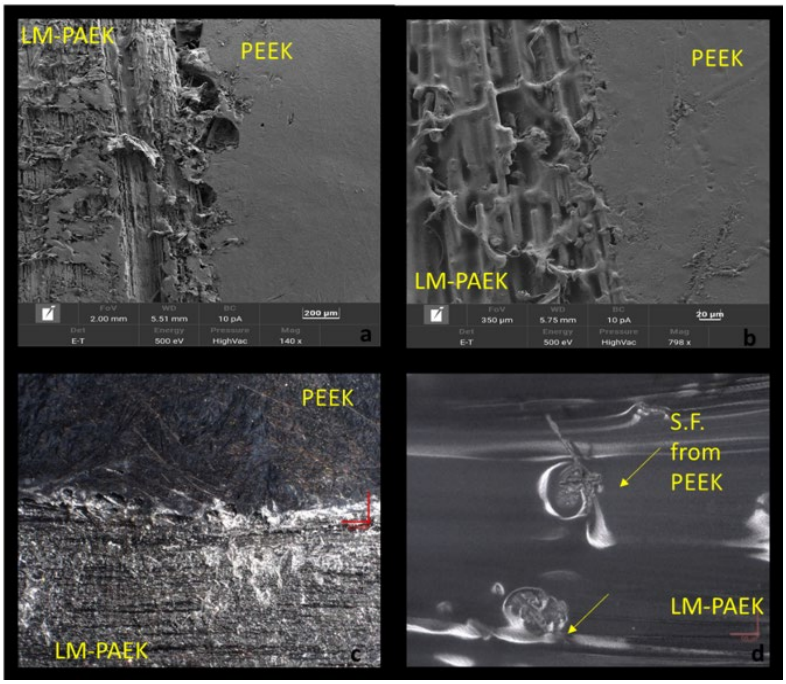

Fig. 7. a, b) SEM images of cross-section (350ºC), c, d) images from optical microscope of cross-section and LM-PAEK side surface after DCB tests.

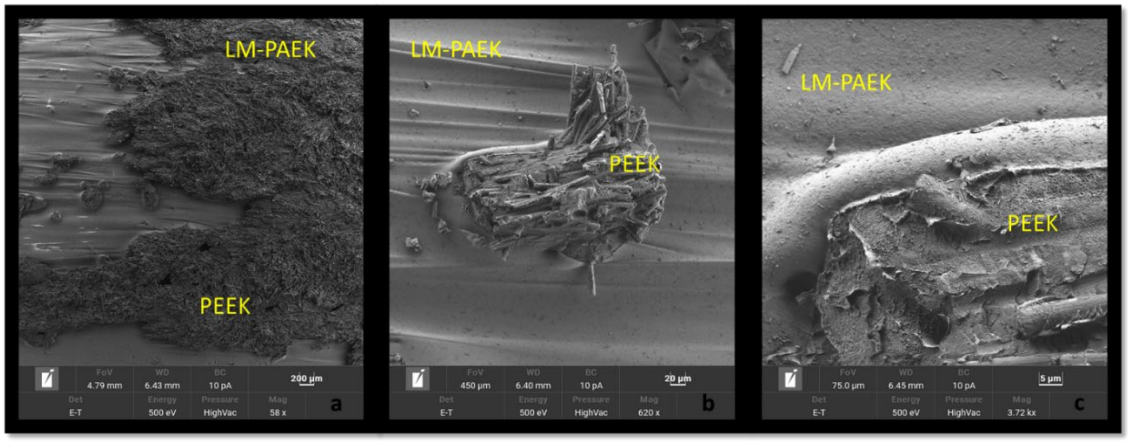

Fig. 8. SEM images of LM-PAEK side surface after DCB test (350ºC).

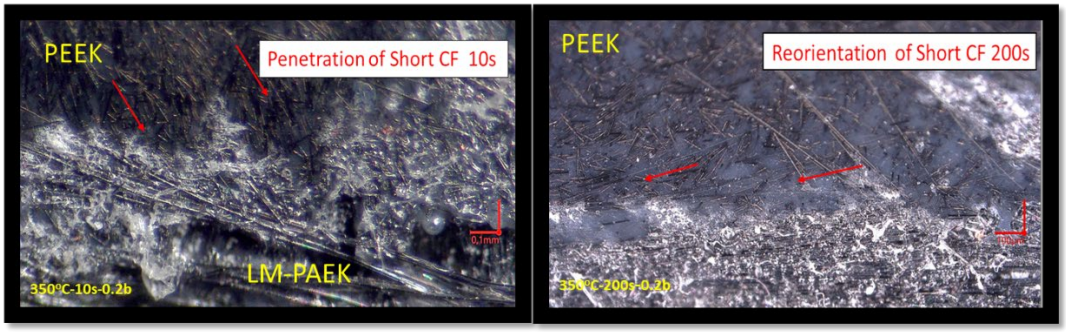

Fig. 9. Optical micrographs of cross-section (350ºC) for a) 10 s, b) longer contact times (200s).

Conclusion

This study demonstrated the feasibility of welding dissimilar thermoplastic composites-short carbon fiber reinforced PEEK and continuous carbon fiber reinforced LM-PAEK-using a rapid conductive heating technique. The interfacial fracture toughness G_{IC} was shown to be strongly governed by welding temperature and contact time. While the interface temperature exceeded the melting

temperature of LM-PAEK and approached or exceeded that of PEEK, optimal interfacial performance was achieved at 350 °C combined with short-to-intermediate contact times.
Prolonged holding durations led to a reduction in fracture toughness, which was attributed to the reorientation of short carbon fibers within the molten PEEK matrix. At short contact times, these fibers acted as mechanical bridges across the interface, enhancing load transfer at crack initiation. At longer times, fiber alignment parallel to the interface suppressed this bridging mechanism, resulting in lower measured G_{IC} values.
These findings highlight the strong coupling between thermal conditions, holding duration, and interfacial morphology in hybrid thermoplastic systems, particularly when processing occurs near the melting temperature of the higher-melting matrix. The results emphasize the decisive role of short fiber behavior at the welding interface and demonstrate that interfacial performance in dissimilar reinforced thermoplastics is controlled by microstructural evolution.
Beyond establishing feasibility, the present work represents a first systematic step toward understanding welding mechanisms in asymmetric thermoplastic composite joints. The absence of dedicated fracture methodologies for bi-material thermoplastic systems and the instability of crack propagation observed in this configuration underline the need for adapted testing protocols and future standardization efforts. Further investigation into pressure effects, thermal gradients, and fiber orientation dynamics will be essential to establish robust process–structure–property relationships and to enable the reliable industrial implementation of welding strategies for dissimilar reinforced thermoplastic composites.

Acknowledgement

The authors would like to thank Jérôme Delmas and Nicolas Lefevre for their help for their contribution to the design and machining of the welding setup and Samuel Branchu for his valuable assistance with the SEM characterization. The authors also acknowledge the funding of the CONNECT project managed by the IRT Jules Verne (French Institute for Research and Technology) that made this work possible. The authors wish to associate the industrial partners of the CONNECT project: Airbus Atlantic, Airbus Operations, Daher Aerospace, Latecoere, Liebherr Aerospace Toulouse and Cero.

References

[1] J. Audoit, L. Rivière, J. Dandurand, A. Lonjon, E. Dantras, C. Lacabanne, Thermal mechanical and dielectric behavior of poly (aryl ether ketone) with low melting temperature, Journal of Thermal Analysis and Calorimetry, 135(4) (2019) 2147–2157.

[2] L. B. Nohara, M. L. Costa, M. A. Alves, M. F. K. Takahashi, E. L. Nohara, M. C. Rezende, Processing of high-performance composites based on PEEK by aqueous suspension prepregging, Materials Research, 13 (2010) 245–252.

[3] J.P. Reis, M.F.S.F. de Moura, Mixed-mode I+II fracture behaviour of thermoplastic composites and their adhesive bonded joints, Composites Science and Technology, 271 (2025)111349.

[4] J. Avenet, T. A. Cender, S. Le Corre, J.-L. Bailleul, A. Levy, Experimental correlation of rheological relaxation and interface healing times in welding thermoplastic PEKK composites. Composites Part A, 149 (2021) 106489.

[5] J.-N. Dai, S.-Q. Kou, High-content continuous carbon fibers reinforced PEEK matrix composite with ultra-high mechanical and wear performance at elevated temperature, Composite Structures, 295 (2022) 115837.

[6] W. Zhao, R. Yu, W. Dong, J. Luan, G. Wang, H. Zhang, et al., The influence of long carbon fiber and its orientation on the properties of three-dimensional needle-punched CF/PEEK composites, Composites Science and Technology, 203 (2021) 108565.

[7] P. Wang, B. Zou, S. Ding, C. Huang, Z. Shi, Y. Ma, et al., Preparation of short CF/GF reinforced PEEK composite filaments and their comprehensive properties evaluation for FDM-3D printing. Composites Part B: Engineering, 198 (2020) 108175.

[8] W. I. Lee, G. S. Springer, A Model of the Manufacturing Process of Thermoplastic Matrix Composites. Journal of Composite Materials, 21(11) (1987) 1017–1055.

[9] C. Ageorges, L. Ye, M. Hou, Advances in fusion bonding techniques for joining thermoplastic matrix composites: A review. Composites Part A: Applied Science and Manufacturing, 32(6) (2001) 839–857.

[10] J. Avenet, A. Levy, J.-L. Bailleul, S. Le Corre , J. Delmas, Adhesion of high-performance thermoplastic composites: Development of a bench and procedure for kinetics identification, Composites Part A 138 (2020) 106054.

[11] S. Samborski, A. Gliszczynski, J. Rzeczkowski, N. Wiacek, Mode I Interlaminar Fracture of Glass/Epoxy Unidirectional Laminates. Part I: Experimental Studies. Materials 12 (2019) 1607.